Application of agent-based modelling for selecting configuration of vertical slot fishway

Kulić, Tin; Lončar, Goran; Kovačević, Martina; Fliszar, Robert

Primljen / Received: 9.2.2021.
Ispravljen / Corrected: 25.2.2021.
Prihvaćen / Accepted: 28.2.2021.
Dostupno online / Available online: 10.4.2021.

Application of agent-based modelling for selecting configuration of vertical slot fishway

Authors:

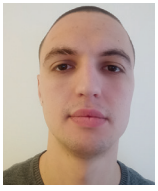

Tin Kulić, MCE
University of Zagreb
Faculty of Civil Engineering
tin.kulic@grad.unizg.hr
Corresponding author

Prof. **Goran Lončar**, PhD. CE
University of Zagreb
Faculty of Civil Engineering
goran.loncar@grad.unizg.hr

Martina Kovačević, MCE
University of Zagreb
Faculty of Civil Engineering
martina.kovacevic@grad.unizg.hr

Robert Fliszar, MCE
University of Zagreb
Faculty of Civil Engineering
robert.fliszar@ grad.unizg.hr

Subject review

Tin Kulić, Goran Lončar, Martina Kovačević, Robert Fliszar

Application of agent-based modelling for selecting configuration of vertical slot fishway

Physical and 3D numerical hydrodynamic flow models and an agent-based model are developed with the principal objective of analysing fish behaviour in two vertical slot fishway configurations. Fish energy consumption due to swimming represents a crucial criterion for selecting an appropriate fishway configuration. The modelled fish detects ambient flow conditions, makes decisions based on its sensing and cognitive abilities, adapts to the changes in its environment, and moves toward the regions of less turbulent kinetic energy. The results show that fishways with longer pools enable passage of fish at a lower energy consumption.

Key words:
fishway, physical model, numerical model, agent-based model

Pregledni rad

Tin Kulić, Goran Lončar, Martina Kovačević, Robert Fliszar

Izbor oblika riblje staze s vertikalnim otvorima na temelju primjene ABM modela

Uspostavljen je fizikalni i 3D numerički model strujanja te model baziran na agentima (eng. Agent-Based Model - ABM) za potrebe praćenja prolaska ribe kroz dvije konfiguracije riblje staze s vertikalnim otvorima. Potrošnja vlastite energije ribe pri prolasku kroz riblju stazu predstavlja ključni parametar ocjene o kvaliteti pojedine konfiguracije riblje staze. Modelska riba prepoznaje okolišne uvjete pomoću svojih senzorskih sposobnosti te donosi kognitivne zaključke o promjeni smjera kretanja prema zoni manje turbulentne kinetičke energije. Rezultati provedenog istraživanja pokazali su da riblja staza s duljim bazenima omogućuje prolazak ribe s manjim utroškom energije.

Ključne riječi:
riblja staza, fizikalni model, numerički model, ABM model

Übersichtsarbeit

Tin Kulić, Goran Lončar, Martina Kovačević, Robert Fliszar

Auswahl der Form eines Fischpfades mit den vertikalen Öffnungen, aufgrund der Anwendung des ABM-Modells

Es wurde das physikalische Modell, sowie das nummerische 3D-Modell der Strömung, genauso wie das Modell, welches sich auf den Agenten gründet (in englischer Sprache: Agent-Based-Modell- ABM), und zwar für den Bedarf der Begleitung von Fischen durch zwei Konfigurationen eines Fischpfades mit den vertikalen Öffnungen hergestellt. Der Verbrauch der eigenen Energie des Fisches durch den Fischpfad stellt einen Schlüsselparameter der Bewertung über die Qualität der einzelnen Konfiguration eines Fischpfades dar. Der Modellfisch erkennt die Umweltbedingungen mittels seiner sensorischen Fähigkeiten, und er zieht kognitive Schlussfolgerungen über die Änderung der Bewegungsrichtung in die Richtung der Zone mit der kleineren turbulenten kinetischen Energie. Die Ergebnisse der durchgeführten Forschung haben gezeigt, dass ein Fischpfad mit dem längeren Pfad den Durchgang des Fisches mit dem kleineren Energieverbrauch ermöglicht.

Schlüsselwörter:
Fischpfad, das physikalische Modell, das nummerische Modell, das ABM-Modell

1. Introduction

Climate change, environmental degradation, loss of biodiversity, and similar topics, have been increasingly debated in many research papers, various expertise studies, and discussions, as the extremely negative consequences of human-related activities. Accordingly, the interruption of river continuum stands out as one of such unfavourable activities that affect ecosystems related to watercourses. Barrier construction along watercourses (such as hydroelectric power plants, dams, weirs, etc.) has a significant effect on many ecosystem users, especially fish and their migration cycle. An increase in environmental preservation awareness and usage of renewable energy resources has led to a surge in the construction of small hydropower plants. Such facilities have a less negative impact on preservation of river continuum and biodiversity [1]. This paper focuses on the upstream fish migration through a fishway with the smallest possible energy consumption. However, damage to fish and exposure to predators are disregarded [2].

The fishway is a canal designed to obtain such hydraulic flow conditions that fish consider favourable in their upstream or downstream migrations. These engineering facilities are divided into two main groups: technical and natural fishways [3]. This research includes the analysis of a technical vertical slot fishway, as discussed in Section 2 Materials and methods. Fishway design should be adjusted according to the physical characteristics of fish with an emphasis on adapting the flow conditions to the abilities of the weakest swimmer [3]. Hence, fish have to overcome critical fishway sections where maximum flow velocities occur (flow contraction at the location of vertical slots). To swim against the water current in areas of maximum velocities, fish use their burst speed that can be maintained for a few seconds, what requires a certain recovery time afterwards. Burst speed for fish families *Salmonidae*, *Percidae* and those belonging to the order of *Cypriniformes* varies between 10 and 12 body lengths per second (BL/s). Furthermore, a prolonged fish speed which ranges between 3 and 5 (BL/s), needs to be obtained in the other parts of the fishway [3-6].

Numerous natural and anthropogenic factors that affect fish swimming capability have been discussed in numerous studies. Beamish [5] highlights the water temperature and dissolved oxygen concentration in water as two main factors that negatively affect the prolonged fish speed. Several authors have revealed that the vortex size and turbulence intensity stand out as two hydrodynamic factors that affect fish swimming capability [6-12]. Although turbulence is usually addressed in a negative context when considering its influence on fish swimming, Liao [7, 8] examined the movement pattern used by fish to harness the energy of environmental vortices in turbulent flows in order to minimize their energy consumption. Also, he elaborated on the relationship between the vortex and fish sizes in turbulent flow. If body length is more than an order of magnitude larger than the vortex size, fish swims steadily through it, and vice versa. Hockley et al. [13] state that fish tend to avoid water currents with significant velocity fluctuations, and that their ability to overcome turbulent flow is mainly related to body length, weight, and shape. A more detailed analysis of the relationship between the fish body length, swimming capability, and vertical slot fishway design, is presented by Cai et al. [14]. They examined the behaviour of seven target species that weighed between 10 and 400 [g] with a body length between 5 and 40 [cm]. Their research resulted in recommendations for the flow velocity criteria that should be considered in the vertical slot fishway design. Fish [15] and McKenzie [16] focus on the topic of the energetics of fish swimming. They note that fish tend to use burst velocity even when low velocities with small fluctuations occur, i.e. in flow conditions that could be overcome by using prolonged speed. Furthermore, they present a common equation for calculating the fish drag power. It is obtained from the relation for the hydrodynamic drag force as a function of the fish body size, water density, and flow velocity. Also, the equation is used in this paper for calculating the rate of fish energy loss due to swimming.

Fishway configuration plays an important role in ensuring the river continuum. Quality fishway design enables successful fish migrations along watercourse sections where flow discontinuities occur. Flow conditions in fishways are usually examined using physical models in laboratories. In such a way, it is possible to adjust the model geometry relatively fast and obtain results efficiently for various configurations. The Particle Image Velocimetry (PIV) for recording the flow velocity field has been applied successfully in fishways with various slopes, inflows, and widths [17]. Silva et al. [9] observed behaviour of Iberian barbel (*Luciobarbus bocagei*) in an experimental pool-type fishway with a constant slope, variable inflow, and submerged orifice. Flow velocities were measured continuously with a 3D Acoustic Doppler Velocimeter (ADV) while the fish movement was recorded with a video camera. The conclusion was that Iberian barbel occupies the areas with low turbulent kinetic energy (TKE), i.e. with low turbulence. Adults of this species showed a higher rate of passage success when compared to smaller-size individuals. Bermudez et al. [18] analysed movement of brown trout (*Salmo trutta*), Iberian straight-mouth nase (*Pseudochondrostoma polylepis*), and Iberian barbel. They presented recirculation zones where low turbulence and velocities occur within vertical slot fishways. These zones are usually designed as resting areas and the study showed that fish stay most frequently behind baffles just downstream of the slot. Furthermore, fish trajectories were defined and presented for the narrow area upstream and downstream of the slot. The authors concluded that fish mostly used the area behind the smaller lateral baffle before transiting to the upstream pool. Li et al. [19] analysed velocity field in two

vertical slot fishways for various slopes and baffle shapes. Flow velocity was measured continuously with ADV. Also, a 3D hydrodynamic model was developed and verified based on the observed velocities. It was concluded that baffle shape greatly influences the flow pattern, i.e. TKE, energy dissipation rate, and vorticity. Furthermore, it was concluded that the flow velocity, TKE, and energy dissipation rate are positively correlated with fishway slope. The water level difference between adjacent pools was identified as the main factor affecting maximum velocities at vertical slots. This conclusion was found very useful from the economic point of view as it enables the construction of shorter fishways with steeper slopes can be built.

The methodology used in previous studies is also applied in this research paper. A 3D hydrodynamic model of vertical slot fishways was developed, and model simulations were verified based on the observations from the corresponding physical models. The hydrodynamic model is coupled with a fish swimming model, which constitutes a contribution of this research.

Fish are complex animals with a highly developed ability for prey capturing, avoiding predators and detecting environmental conditions favourable for their growth and spawning. Therefore, a cognitive aspect plays an important role in the fish swimming model, and should be included in the mathematical formulation of the problem, along with physical elements of the process. The formulation of the behaviour of individuals that is adaptable to environmental conditions represents the core of the Agent-Based Model (ABM) simulations [20, 21].

Agent-based modelling is a relatively new approach in investigating the individuals that mutually interact and adapt their behaviour based on changes in their environment [22]. ABM procedures focus on the description of actions and interactions between individuals (agents) and the environment, instead of describing a fully modelled global phenomenon [23]. The purpose of ABM development also defines its complexity.

This paper presents an original ABM of fish swimming through fishway developed using the ecological modelling software ECOLab within the MIKE numerical modelling framework (www.dhigroup.com). The modelling aspects that have been considered within this ABM include a physical component involving application of a hydrodynamic model (flow model with the extracted TKE scalar field) coupled with a behavioural component (fish swimming upstream to the zone of increased hormone concentration while avoiding the areas of intensive TKE). Biological components - growth and mortality, and changes in temperature and dissolved oxygen concentration have been neglected due to the short time the fish (agent) spends in the fishway. Lastly, the movement of individual fish is examined for various fishway configurations.

The authors of this paper were unsuccessful in finding previous studies related to the coupled hydrodynamic models and ABM of fish swimming through fishway (Eulerian approach for flow field and Lagrangian model for the analysis of fish movement). Earlier studies do not quantify the time-dependent fish energy consumption for different fishway configurations. Also, previous studies present the coupled hydrodynamic models with ABMs intending to solve the problem of fish finding the fishway entrance [24-26], fish migrations in river estuaries [27], and seasonal migrations of fish in seas [28]. Fish trajectories that follow the agents from their source location in the watercourse to the fishway entrance were extracted in papers [24-26] . However, the analysis of fish swimming upstream through the fishway was not conducted.

The first part of Section 2 includes a description of datasets used for developing a physical model of the fishway and measurements of flow depth and velocity for two configurations. The development of the numerical flow model of fishways and presentation of the verified model results are given in the second part of the same section. The third part of Section 2 offers a detailed description of the ABM of fish swimming through fishway as well as specifications of ABM simulations. The ABM simulation results are presented in Section 4, and conclusions are given in Section 5.

2. Materials and methods

2.1. Physical model of the fishway

The physical model of the fishway was built in form of a glass rectangular flume in the Hydrology and Hydraulics Laboratory of the Department for hydrosciences and engineering of the Faculty of Civil Engineering, University of Zagreb (Figure 1). The flume is 1 [m] in width, 18 [m] in total length, out of which 13 [m] is the working length. The water in the flume recirculates and is captured from the underground canal with a low-pressure pump (KSB AMAREX N). The discharge is regulated by a gate valve that is installed upstream of the electromagnetic flowmeter (Enders+Hauser Promag 53). A controlled weir is installed at the flume outlet (Figure 1).

Two configurations of vertical slot fishways are built in a flume (Figure 2). The total width, length, and bed inclination values are the same for both configurations and amount to (45 [cm], 3 [m], and 13 [%], respectively. Model baffles are made of waterproof plywood. The fishway configurations are defined with a pool distance, i.e. the distance between main baffles. The distance for the first configuration is 90 [cm], while in the second configuration this distance is equal to 45 [cm] (Figure 2). For simplicity, the fishway with pools that are 90 [cm] long will be described as RS-90, will be described as RS-90 and the second configuration as RS-45.

Velocities were recorded in the mid pool using the ADV device (VECTRINO CABLE PROBE 10MHz) at 9 measuring points (Figure 2) for three levels (at the surface, in the middle of

the water column, at the bottom, 27 points in total). Each measuring point involved data recording in 2-minute time intervals, with a sampling frequency of 5 [Hz]. The discharge at the flume inlet was set to Q = 20 [l/s]. The water level at the upstream boundary was set to 65 [cm] for RS-90 and 71 [cm] for RS-45. At the downstream boundary, the water level was maintained at 25 [cm] for both configurations. Flow velocity results obtained at the measuring points are compared with numerical simulation results in Section 3 Results and discussion. This physical model is a pilot model that does not represent a downscaled existing fishway.

Figure 1. Glass flume (canal) at the Hydrology and Hydraulics Laboratory of the Water Research Department (left, looking upstream), and controlled weir at the canal outlet (right) [3]

2.2. Numerical model of the fishway

The numerical flow model of the fishway should provide information about key physical processes that affect the cognitive response of fish during their upstream migration through this structure. For instance, it should provide an image of zones with intensive vorticity and/or turbulence that fish can detect and make decisions based on the changes in their environment. A 3D hydrodynamic flow model MIKE 3FM, which is based on the finite volume method, was developed in the scope of this research. Spatial discretization and model mesh is shown graphically below only for the fishway with a pool length of 90 [cm] as the other configuration, i.e. RS-45 is similarly defined with the same density of mesh elements (Figure 3). The horizontal model domain is described with an unstructured mesh of finite volumes where the distance between the elements' centroids varies between 0.005 [m] and 0.02 [m]. The model is forced with a constant discharge of Q = 20 [l/s] at the upstream boundary, which corresponds to the discharge set at the physical model inlet. The downstream boundary condition is defined as a constant water level observed at the physical model outlet (25 [cm] for both configurations). By varying the value of the absolute model roughness up to the point of obtaining the values of water level measured at the physical model inlet (65 [cm] for RS-90, 70 [cm] for RS-45), a constant absolute roughness value of 0.0002 [m] is adopted for canal bed and walls. The vertical domain of the model is described with 5 σ-layers as such discretization has proven to be the most effective in terms of reducing the computation time with acceptable model accuracy. It is important to note that the sensitivity analysis of model results has also been made. It is based on the variable number of σ-layers. For instance, differences in the modelled TKE field vary less than 3 % for 15, 10 and 5 σ-layers. In the case when the model is vertically discretised with 4 σ-layers and 3 σ-layers, the differences of the same parameter (TKE) increase to 12 % and 35 %, respectively.

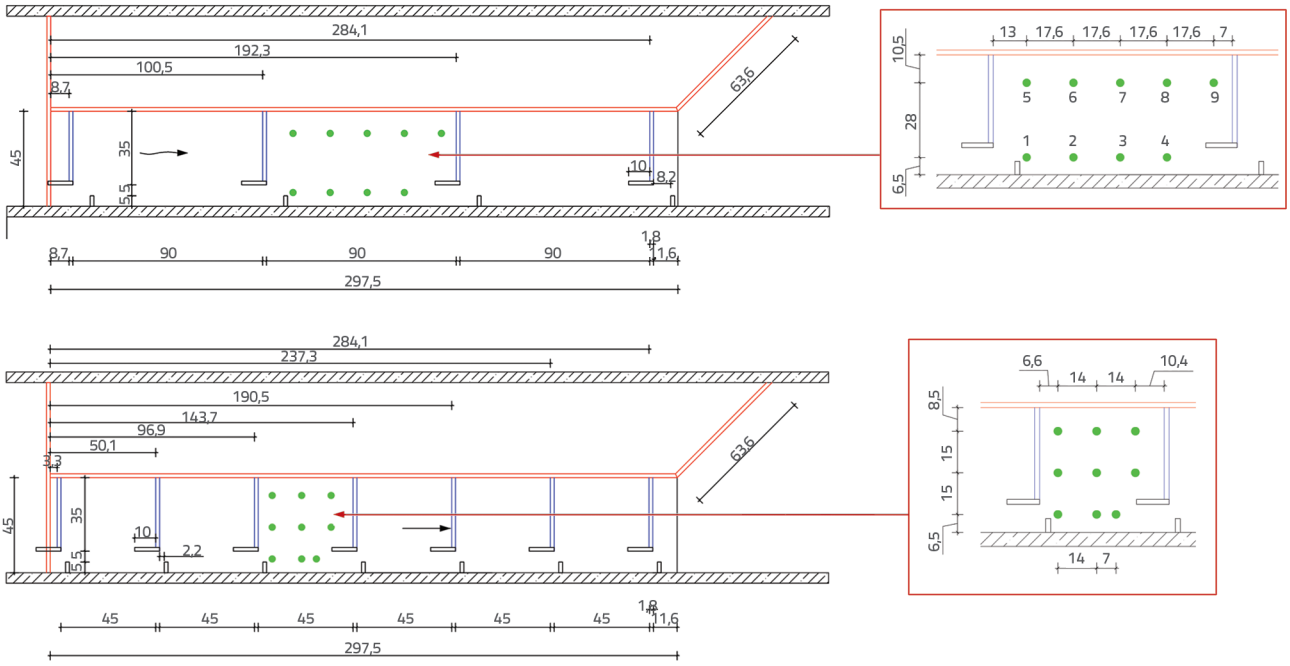

Figure 2. Geometry (ground plan) of the analysed physical models of vertical slot fishway (left) and disposition of measuring points (right)

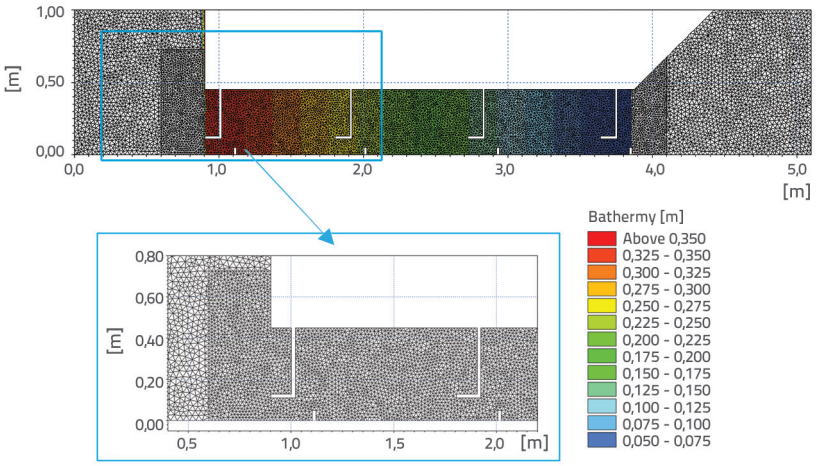

Figure 3. Model spatial domain for RS-90 configuration and unstructured triangular finite volume mesh

The turbulence model is defined by the *k*-ε formulation in vertical [29] and the Smagorinsky concept in horizontal direction [30]. The Smagorinsky coefficient is used as one of the calibration parameters and a constant value of 0.1 is adopted when discrepancies of the measured and modelled velocities have been minimized. The calibration procedure and comparison of measurements and simulations are explained in detail in Section 3. Scaling factors for the turbulent kinetic energy (*TKE*) and its dissipation rate (ε) are equal to 1 and 1.3 in the horizontal and vertical directions, respectively. The variable computational time step depends on the mesh element size regulated by the CFL (Courant-Friedrichs-Lévy) parameter limited to the value of 0.8.

The velocity and TKE fields, obtained by the hydrodynamic flow model, are used as the basis for the ABM of fish swimming through the fishway. In its upstream movement along the fishway, fish is attracted by a higher ambient hormone concentration, avoiding the zones of high TKE. This cognitive component of fish behaviour represents the essence of the developed ABM.

2.3. ABM development and simulations

Numerical simulations included analysis of the movement of fish of an assumed length of 25 [cm] and the ability to reach the speed of 2.5 [m/s] in burst mode swimming and a continuous speed of 1.1 [m/s]. The values were derived from previous studies presented in papers [3-6] and have already been discussed in Section 1 Introduction. Hence, the modelled fish corresponds to the rainbow trout (*Salmo gairdneri*) [31]. In the text that follows, the term agent denotes an individual fish.

ABM simulations were conducted based on the velocity and TKE fields that were extracted from verified results of the hydrodynamic flow model. The basic concept of the developed ABM is presented below.

Fish energy (*E*) represents the ABM state variable based on the following expression [15, 16]:

$$\frac{dE}{dt} = -0.5\rho_v C_b v_{agent,rel}^3 \ [J] \qquad (1)$$

where (ρ_v) is the water density [kg/m^3], (C_b) is the dimensionless drag coefficient, ($v_{agent,\ rel}$) is the target fish speed [m/s] (relative fish speed), i.e. the speed that fish tends to reach considering ambient conditions affecting its movement (flow velocity, turbulence). When swimming collinearly with the water current, fish reduces its relative speed and uses the flow energy for moving upstream. Such movement pattern enables the agent to save energy and use it later for overcoming the areas of highest flow velocities (flow contractions at vertical slots). When swimming against the water current, the agent adaptively uses its continuous or burst swimming speed depending on the ambient flow. The upstream movement of the agent stops when available energy reaches the limit of 0, i.e. the fish is carried away with water current towards downstream fishway sections when condition E = 0 is satisfied. The core of the fish movement motivation is related to the hormone concentration field that monotonously increases in the upstream direction. Also, fish avoids zones of intensive TKE.

A detailed description of ABM components for fish movement is provided in the following text. In terms of this research, ABM components are constants, agent sensing functions, and mathematical expressions for describing behavioural and physical fish characteristics.

The constants, used within this ABM, are water density (ρ_v) = 1000 [kg/m^3], fish length (L) = 0.25 [m], continuous swimming speed ($v_{agent,C}$) = 1.1 [m/s] which is equivalent to 4.4 [BL/s], burst swimming speed ($v_{agent,B}$) = 2.5 [m/s], which corresponds to 10 [BL/s].

Sensing functions are described by two functions incorporated in the software. Both functions are used for the determination of the relative agent movement direction. The first function ($\theta_{min,TKE}$) is used for movement to minimum TKE based on the detection of an ambient 2D TKE field within the radius of 0.018 [m]. This approach involving the agent's tendency to move towards lower TKE is derived from previous studies shown in [7, 8, 13, 18]. The second function ($\theta_{max,WILL}$) is related to the determination of the movement towards higher hormone concentrations based on the ambient 2D hormone field detection within the same search radius. A diagram describing the principle of sensing functions is provided below for the fish movement towards the minimum TKE in its ambient.

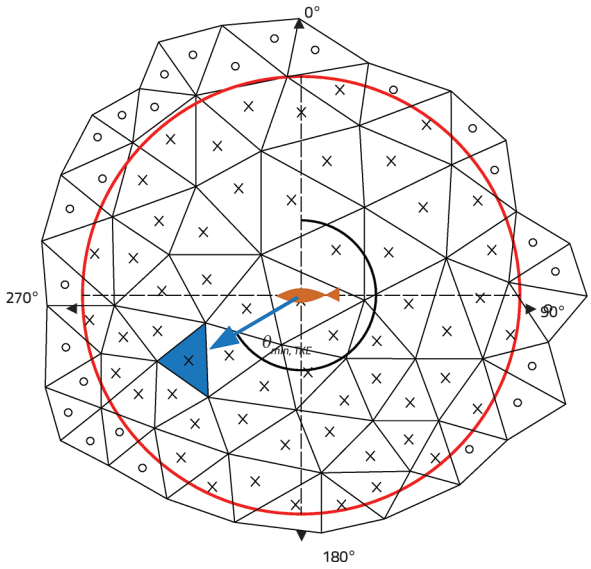

Figure 4. Diagram of agent's detection of and movement towards minimum TKE in its ambient according to [32]

Note: The orange symbol represents the current location of the agent, blue triangle the mesh element with minimum TKE, red circle the boundaries within the agent's search radius, crossed element centroids the mesh elements that the agent detects, and circular element centroids the mesh elements that agent is unable to detect during its movement.

In the area of the denser unstructured mesh, the agent detects four nearest elements with the corresponding TKE and hormone concentration values within its search radius. On the contrary, in the zones of the less dense model mesh, the agent detects only one closest element.

Arithmetic expressions defined during the development of ABM are described below. The flow area (A) of fish is given by [4]:

$$A = 0{,}4 \cdot L^2 \ [m^2] \tag{2}$$

The agent's relative movement direction ($\theta_{agent,rel}$), based on the modelled 2D fields of flow direction and TKE, is given by the following formulation:

$$\theta_{agent,rel}\left[m/s\right] = \begin{cases} \varphi_{HD,h}, & \sin\left(\varphi_{HD,h}\right) < 0 \wedge \left|\sin\left(\varphi_{HD,h}\right)\right| > \left|\cos\left(\varphi_{HD,h}\right)\right| \\ \theta_{\min,TKE}, & \sin\left(\varphi_{HD,h}\right) < 0 \wedge \left|\sin\left(\varphi_{HD,h}\right)\right| < \left|\cos\left(\varphi_{HD,h}\right)\right| \\ -\varphi_{HD,h}, & \sin\left(\varphi_{HD,h}\right) > 0 \wedge \left|\sin\left(\varphi_{HD,h}\right)\right| > \left|\cos\left(\varphi_{HD,h}\right)\right| \\ \theta_{\min,TKE}, & \sin\left(\varphi_{HD,h}\right) > 0 \wedge \left|\sin\left(\varphi_{HD,h}\right)\right| < \left|\cos\left(\varphi_{HD,h}\right)\right| \end{cases} \tag{3}$$

where ($\varphi_{HD,h}$) is the direction of the water current vector in horizontal plane that is extracted from the results of the hydrodynamic flow model. A schematic of the agent's decision making regarding its movement direction, based on the ambient hydrodynamic conditions, is provided at Figure 5.

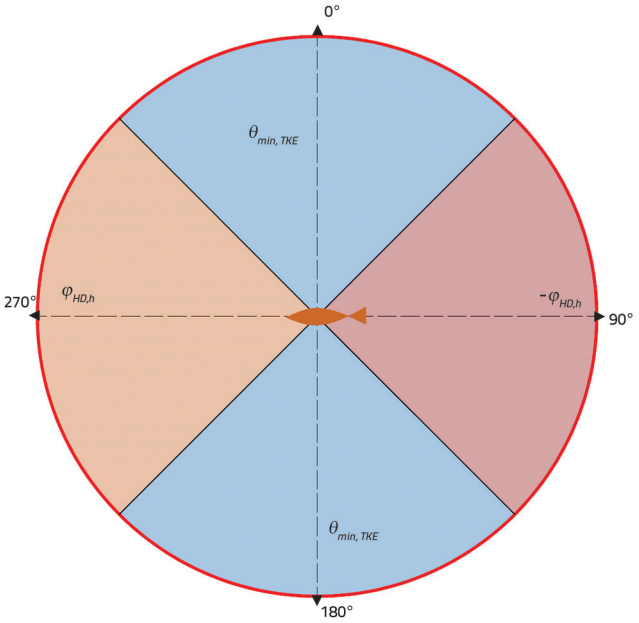

Figure 5. Schematic of the agent's decision on movement direction based on the ambient hydrodynamic conditions (flow direction, TKE)

The agent's target movement speed ($v_{agent,rel}$), based on the modelled 2D fields of flow direction and velocity that are extracted from the hydrodynamic model, is described by the following formulation:

$$v_{agent,rel}\left[m/s\right] = \begin{cases} v_{HD,h}, & \sin\left(\varphi_{HD,h}\right) < 0 \wedge v_{HD,h} > 0{,}2 \\ v_{agent,C}, & \sin\left(\varphi_{HD,h}\right) < 0 \wedge v_{HD,h} < 0{,}2 \\ v_{agent,B}, & \sin\left(\varphi_{HD,h}\right) > 0 \wedge v_{HD,h} > 0{,}9 \\ v_{agent,C}, & \sin\left(\varphi_{HD,h}\right) > 0 \wedge v_{HD,h} < 0{,}9 \end{cases} \tag{4}$$

where ($v_{HD,h}$) represents the flow velocity in horizontal plane obtained from the hydrodynamic model. The agent's decision regarding the swimming mode that will be used (continuous or burst) is defined based on the threshold values of ($v_{HD,h}$). These thresholds are derived and adjusted according to results presented in [14].

The dimensionless fish drag coefficient (C_b) is assumed to be dependent on the ($v_{HD,h}$), as presented in the expression below:

$$C_b\left[1\right] = \begin{cases} 10, & v_{HD,h} < 0{,}2 \\ 30, & 0.2 < v_{HD,h} < 0{,}9 \\ 150, & v_{HD,h} > 0{,}9 \end{cases} \tag{5}$$

where (C_b) is described by increasing the stepwise function. Another assumption is that the adopted (C_b) increases with an increase in the flow velocity and the agent's intention to overcome the flow. Considering that the authors are not familiar with the exact and certain values of (C_b), the previous assumption

leads to the proportional relationship between (C_b) and the target (relative) movement speed of the agent. These assumptions are considered valid in the light of the fact that similar conclusions are made in [15, 16] regarding the relationship between the two described parameters. It is indicated in these studies that (C_b) increases three- to five-fold as a consequence of propulsive movements of the fish. Therefore, if the flow velocity is below 0.2 [m/s], (C_b) is assumed to be 10. If the flow velocity varies between 0.2 and 0.9 [m/s], (C_b) increases three-fold and amounts to 30. For the flow velocity above 0.9 [m/s], (C_b) is equal to 150, which corresponds to the value five times higher than (C_b) for the lower velocity class.

The agent's absolute movement direction (θ_{abs}), which considers both the 2D fields of the outputs from the hydrodynamic model (flow direction and velocity, and TKE) and 2D field of the assumed hormone concentration, is given by the following expression:

$$\theta_{abs} = f\left(v_{agent,rel}, \theta_{rel}, v_{agent,rel}, \theta_{max,WILL}\right)\left[^{\circ}\right] \tag{6}$$

where (θ_{abs}) is a function of ($v_{agent,rel}$), (θ_{rel}) and ($\theta_{max,WILL}$), which determines the final target direction of the agent. The first and second elements given in brackets are related to the magnitude and direction of the first vector, while the third and fourth elements represent the magnitude and direction of the second vector. It is important to note that this function is used to obtain only the agent's resulting movement direction, and so the magnitudes of the two vectors are assumed as equal. In this way, the agent chooses its final movement direction based on hydrodynamic conditions and hormone concentration in its ambient. A schematic for defining the agent's final movement direction is provided in Figure 6.

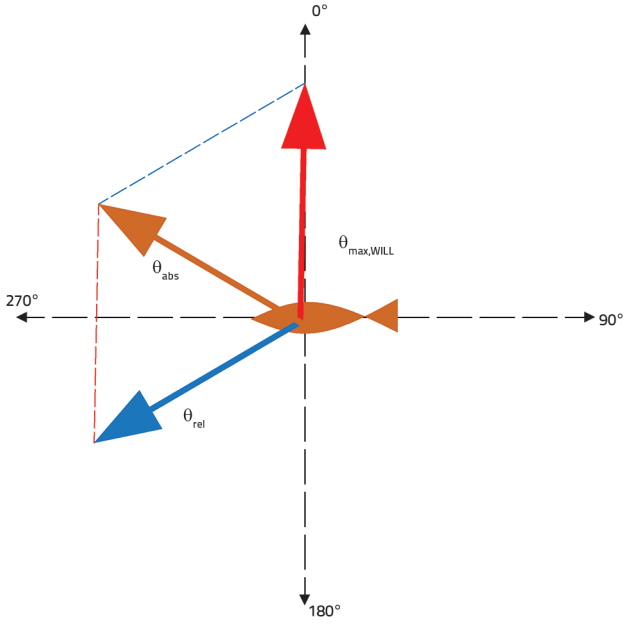

Figure 6. Schematic for defining the agent's final movement direction(θ_{abs})

The agent's absolute or resulting movement speed ($v_{agent,abs}$) is derived from its target speed ($v_{agent,rel}$), its target direction (θ_{abs}), flow velocity ($v_{HD,h}$) and flow direction ($\theta_{HD,h}$):

$$v_{agent,abs} = f\left(v_{agent,rel}, \theta_{abs}, v_{HD,h}, \varphi_{HD,h}\right)\left[\mathrm{m/s}\right] \tag{7}$$

where ($v_{agent,abs}$) is described as a function of ($v_{agent,rel}$), (θ_{abs}), ($v_{HD,h}$) i ($\varphi_{HD,h}$). The first two parameters in brackets represent the agent's relative (target) movement vector, while the other two are related to the flow vector in the horizontal plane. The agent's resulting speed is obtained in a way that is similar to the schematic shown in Figure 6. ($v_{agent,abs}$) differs from the function ($\theta_{agent,abs}$) in the magnitudes of the two vectors, and in the final result of this function, which is the magnitude expressed in [m/s]. In such a way, the water current defies the agent's target movement, i.e. its target speed and direction described with its flow velocity and direction, which gives the resulting vector of the agent's movement. Both ($\theta_{agent,abs}$) and ($v_{agent,abs}$) are in-built software functions, while (6) and (7) represent generalized equations used for describing the framework of the two functions.

The key parameter to be defined in order to calculate the time variability of the state variable – energy (1), is the agent's power (P) which is given by:

$$P\left[W\right] = \begin{cases} 0, & v_{agent,rel}^3 = v_{HD,h} \\ -0{,}5\rho_v C_b v_{agent,rel}^3 & \text{otherwise} \end{cases} \tag{8}$$

where the above equation is derived from the expression for calculation of the fish drag force. The assumption is that (P) is equal to 0 when the agent's relative speed is equal to the flow velocity ($v_{HD,h}$). Considering that the agent uses flow velocity when it moves collinearly with water current (4), the energy loss occurs only when it uses continuous or burst swimming speed. The agent's final movement vector is defined by its components in a horizontal plane and vertical direction. The expressions for horizontal movement direction (9) and speed (10) are presented.

$$\theta_{agent,h}\left[^{\circ}\right] = \begin{cases} \theta_{agent,abs}, & E > 0 \\ \varphi_{HD,h}, & E < 0 \end{cases} \tag{9}$$

$$v_{agent,h}\left[\mathrm{m/s}\right] = \begin{cases} v_{agent,abs}, & E > 0 \\ v_{HD,h}, & E < 0 \end{cases} \tag{10}$$

The final horizontal direction ($\theta_{gent,FIN}$) is equal to the agent's absolute movement direction if the agent has not expended its energy. Otherwise, ($\theta_{agent,FIN}$) is equal to the flow direction if its energy is depleted. Similarly, the final horizontal speed of the agent ($v_{agent,FIN}$) corresponds to the absolute movement speed if its energy is not expended. On the other hand, the total energy consumption leads to the agent being carried away by the water current where its speed corresponds to the flow velocity.

The final link that is necessary for defining the agent's movement vector involves the vertical speed ($v_{agent,V}$), which is given by:

$$v_{agent,V}\left[\text{m/s}\right] = \begin{cases} -v_{HD,V}, & z = 0 \\ v_{HD,V}, & z = d \\ 0, & 0 < z < d \end{cases} \quad (11)$$

where ($v_{HD,V}$) is the vertical flow velocity obtained from hydrodynamic model simulations (positive values are directed from surface to bed), z ϵ [0,d] is the current vertical location of the agent in the water column, and (d) represents the total water depth at the agent's current location. The final vertical speed of the agent corresponds to the negative vertical flow velocity if the agent is at the canal bed (for $z = d$ the agent moves upwards), and to the positive value of the vertical flow velocity when the agent hits the water surface (for $z = d$ the agent moves downwards). If the agent is suspended in the water column, it is assumed that its movement is dominantly present in the horizontal plane, and so ($v_{agent,V}$) is equal to 0 [m/s].

The ABM calibration procedure refers to the development of the original ECOLab template that envelopes all the previously described mathematical expressions and functions. The template has been developed exclusively by the authors of this paper while this software is used as a tool for easier conduct of the simulations and focuses on the understanding of crucial processes. Due to the lack of data about fish swimming patterns through the fishways with similar configurations as the two analysed in this research, the ABM was verified based on previous studies that discuss the topic of fish movement in turbulent flows. Following the previous statement, the fish trajectories presented by Bermudez et al. [18] have been used in this paper for ABM verification, i.e. for the establishment of the final ECOLab template. It is important to note that most of the calibration procedure was related to defining the adequate search radius of the sensing functions. This parameter is related to the model spatial discretization where the final adoption of the radius value of 0.018 [m] leads to a rather smooth fish trajectory throughout the fishway. The increase in search radius causes interruptions in the agent's movement with mostly its retention downstream of the fishway baffles. However, the decrease of search radius leads to the unreasonable chaotic movement of the agent. Both increase and decrease of search radius cause higher energy consumption by the agent for covering the same distance, as well as the irregular shape of the trajectory in its upstream movement. Therefore, the search radius stands out as the most sensitive parameter in terms of final model results regarding the agent's trajectory and energy consumption.

A total of 6 ABM numerical simulations were conducted (Table 1). A half of these simulations relates to the analysis of a model fish swimming through RS-90, and the other half through RS-45 fishway configuration. The initial location of the agent is assumed to be at the fishway entrance, i.e. on half of the downstream model boundary. The simulations differ for the two configurations in the TKE field obtained from the hydrodynamic model simulations, and the depth of the initial agent's location. Such an approach was applied to show the agent's trajectory during its movement through a particular σ-layer. The computational time step is fixed at 0.05 [s].

3. Results and discussion

The depth-averaged flow velocities are presented in Figure 7, while the vertical profile of TKE in the fishway is provided in Figure 8. Comparison of the measured and modelled depth-averaged flow velocities for 9 measuring points (see Figure 2) is given in Figure 9 and Figure 10.

Table 1. ABM simulation sets

Simulation No.	Configuration	2D TKE field	Initial depth of the agent [m]
1	RS-90	5th (surface) σ-layer	0.05
2	RS-45		
3	RS-90	3rd (mid) σ-layer	0.12
4	RS-45		
5	RS-90	1st (bottom) σ-layer	0.22
6	RS-45		

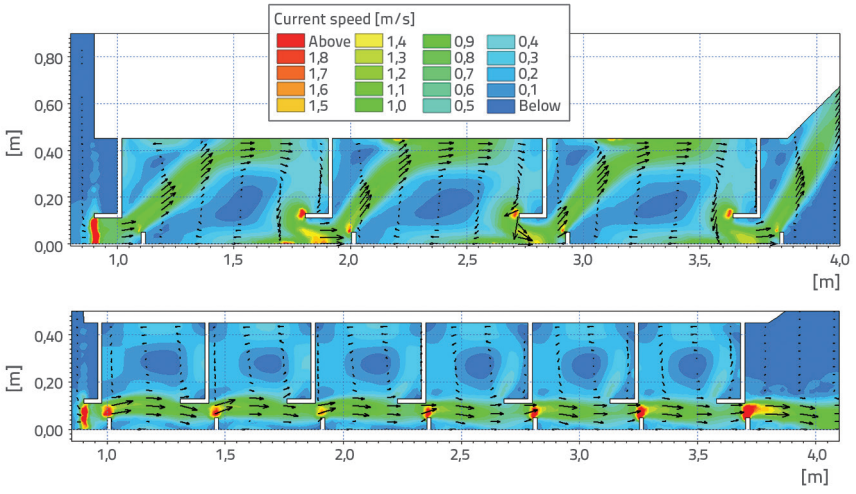

Figure 7. Depth-averaged flow velocity field (up – RS-90, down – RS-45)

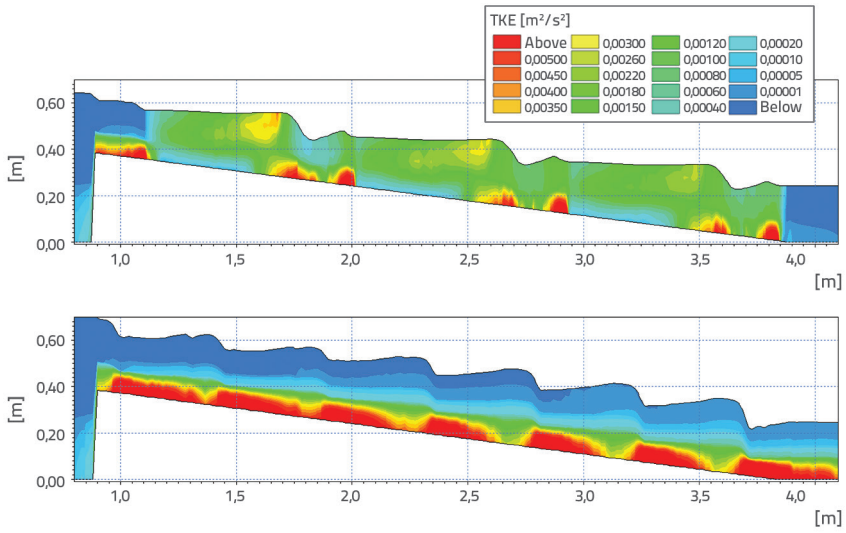

In general, RS-45 is characterised by higher velocities as can be seen in the depth-averaged U and V components as well as in the total current speed presented below (Figure 9, Figure 10). The highest TKE is present at the bottom layer. Furthermore, the vertical section of the TKE in the fishway through vertical slots shows higher turbulence within the RS-45 configuration, i.e. TKE is present more than in the RS-90. However, in the mid and surface layers higher TKE is present for the RS-90 configuration (Figure 8, Figure 11-Figure 13).

Figure 8. Vertical profile of the TKE field in fishway (up – RS-90, down – RS-45)

TKE and flow velocity fields significantly differ depending on the fishway configuration. The main flow is shifted towards the left sidewall for RS-90 while several recirculation zones occur in the pool. On the other hand, the main flow in RS-45 is observed near the right sidewall, while the recirculation zone in the pools extends between the right edge of the vertical slot and the left sidewall. Maximum flow velocities in RS-90 are obtained at the upstream edge of the central (larger) baffle, while for the RS-45 configuration velocities are the highest just downstream of the lateral (smaller) baffle.

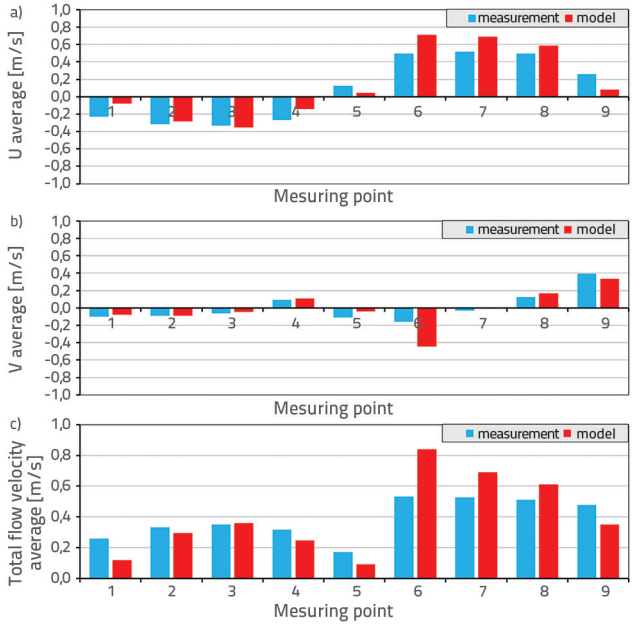

Figure 9. Comparison of measured and modelled depth-averaged U and V components, and total current speed for RS-90 fishway

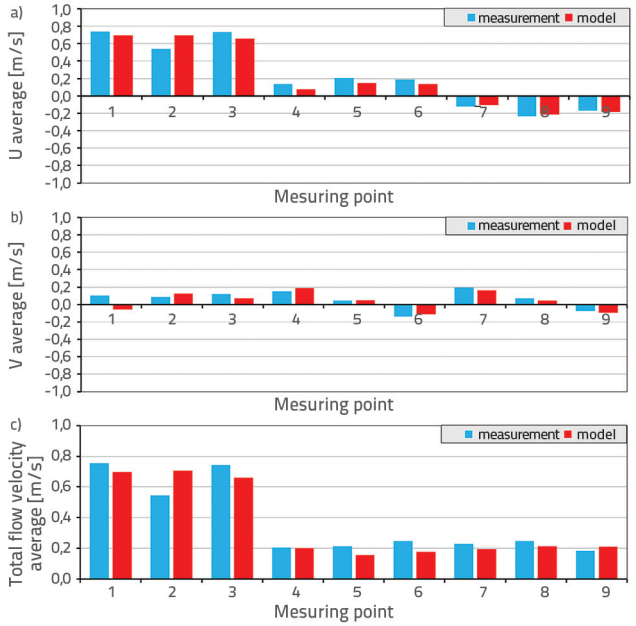

Figure 10. Comparison of measured and modelled depth-averaged U and V velocity components, and total current speed for RS-45

The model calibration included a comparison of the depth-averaged measured and modelled flow velocities for nine measuring points in both fishway configurations (Figure 2). This analysis included calculation of the two statistical parameters for estimating the level of numerical model certainty – mean absolute error Δ_{ABS} (12) and coefficient of determination R^2 (13) [33]:

$$\Delta_{abs} = \frac{1}{n}\sum_{i=1}^{n}\left|y_{model,i}-y_{measured,i}\right| [m/s] \quad (12)$$

Table 2. Statistical parameters Δ_{ABS} and R^2 calculated in the analysis of numerical model certainty for RS-90 and RS-45 fishways

	RS-90			RS-45		
	$U_{average}$ [m/s]	$V_{average}$ [m/s]	Total flow velocity [m/s]	$U_{average}$ [m/s]	$V_{average}$ [m/s]	Total flow velocity [m/s]
Δ_{ABS} [m/s]	0.118	0.060	0.058	0.058	0.043	0.058
R^2	0.910	0.753	0.833	0.962	0.713	0.909

$$R^2 = \frac{\frac{1}{n}\sum_{i=1}^{n}\left(y_{model,i}-\overline{y_{measured,i}}\right)^2}{\frac{1}{n}\sum_{i=1}^{n}\left(y_{measured,i}-\overline{y_{measured,i}}\right)^2}\,[1] \quad (13)$$

where $y_{measured}$ represents measured, and y_{model} modelled U and V components, and the total flow velocity. Parameter i = 1, ..., 9 represents the number of measuring points in the middle fishway pool.

Δ_{ABS} and R^2 of depth-averaged U and V components, and the total flow velocity for both fishway configurations, are presented in the following table.

Based on the obtained flow velocity fields (Figure 7), comparison of the depth-averaged velocities (Figure 9, Figure 10), and calculated statistical parameters, it is evident that the RS-45 model provides results with a higher level of certainty than the RS-90 configuration. Both configurations provide more reliable results for U compared to the V flow velocity component. The most significant error is present for the RS-90 model results when measuring points near the left sidewall are revised (points 6-8, see Figure 2). However, it must be noted that significant turbulence is present in the flow, while the calibration was conducted based on the measurements at several points within the fishway. Also, a general overview of the flow pattern needs to be considered in the model calibration. Accordingly, the modelled flow field corresponds to the ones obtained in previous studies for similarly configured fishways [3, 12, 18, 17, 34, 35].

Figure 11 shows agent trajectories during upstream movement of the agent through the fishway on the background of 2D TKE fields and flow velocity vectors. A trajectory was extracted based on the agent's locations registered every 0.1 [s], i.e. at every second calculation time step. The fish energy loss rate due to upstream movement through the fishway is also presented. A value of 1 [J] is assumed as the initial energy level. The energy loss is presented relatively as a percentage of the agent's available energy for every tenth calculation time step, i.e. at every 0.5 [s]. The initial energy value is assumed arbitrarily because it is rather difficult to measure or estimate the fish energy level at the time it enters the fishway.

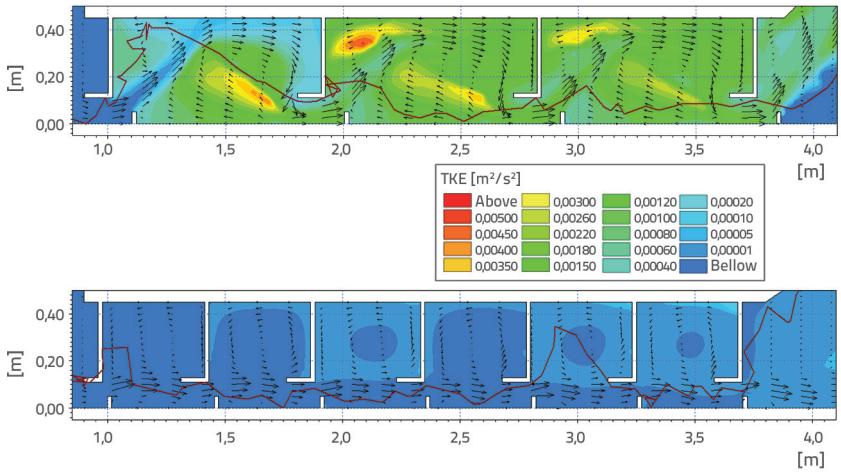

Figure 11. Fish trajectories during upstream movement through the fishways (up: RS-90, down: RS-45) on the background of TKE field and flow velocity vectors in the fifth (surface) σ-layer. The agent is introduced into the fishway at the depth of 0.05 [m]

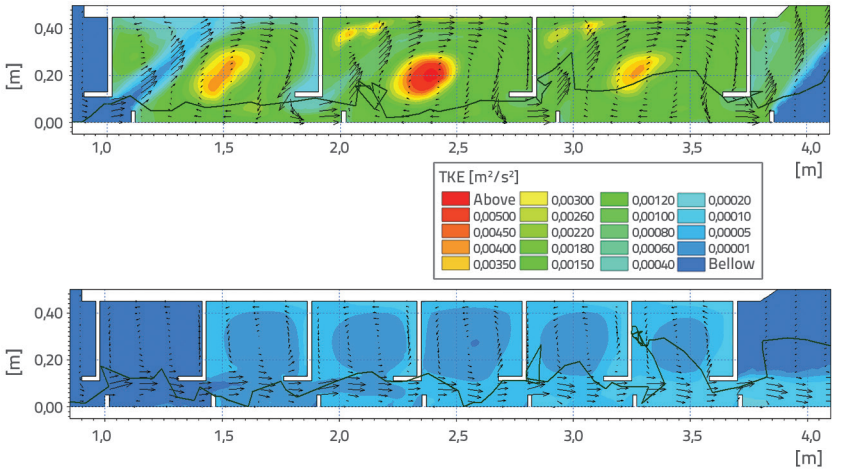

Figure 12. Fish trajectories during upstream movement through the fishways (up: RS-90, down: RS-45) on the background of TKE field and flow velocity vectors in the third (mid) σ-layer. The agent is introduced into the fishway at the depth of 0.12 [m]

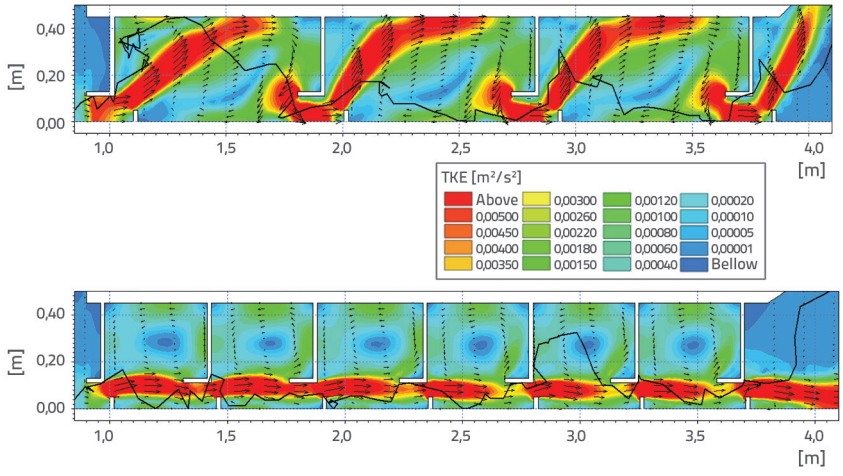

Figure 13. Fish trajectories during upstream movement through the fishways (up: RS-90, down: RS-45) on the background of TKE field and flow velocity vectors in the first (bottom) σ-layer. The agent is introduced into the fishway at the depth of 0.22 [m]

The ABM simulation results were verified based on the movement patterns, reactions, and camera recorded trajectories of fish in altered flows that occur in vertical slot fishways. One of the studies [18] showed that fish can adapt to the ambient flow conditions, i.e. that their movement is adjusted according to the flow speed and direction. The assumption of the adaptive fish behaviour, as related to the change in movement speed based on the change in its environment, confirms one of the fundamental hypotheses of the cognitive fish aspect within the developed ABM.

Fish movement patterns that were investigated earlier in the paper (see Introduction) can be recognized from the ABM simulation results (Figure 11 – Figure 14). The agent avoids the zones with high TKE in its upstream movement, i.e. the fish moves away from turbulent areas. Furthermore, the agent successfully uses burst speed to overcome the zones of high velocities such as flow contraction at vertical slots. On the other side, the agent successfully uses continuous speed during its movement in low-velocity and stable flow zones. Also, in the areas where the flow is collinear with the agent's preferable movement direction, the agent uses the flow to reduce its energy consumption (Figure 14). In the zones of rapid change in flow direction and velocity, the agent moves chaotically as can be seen in the RS-90 configuration results, when the agent moves from the middle to the upstream pool (Figure 13-up).

The agent's more frequent use of the recirculation zones in RS-90 compared to RS-45 results in lower energy consumption for the first configuration. The agent's residence time in the fishway varies between 7 and 14 [s], as can be seen in energy loss diagrams for the two configurations. Also, the agent's time of stay in the RS-90 fishway is shorter (Figure 14). The final time step at the two diagrams represents the moment when the agent leaves the model spatial domain, i.e. when it moves through the upstream model boundary. Considering the above, RS-90 represents a more favourable fishway configuration compared to RS-45. The lowest energy loss occurs when the agent is introduced into and moves through the surface, while the highest energy loss occurs for its movement in the bottom σ-layer. Such an energy loss pattern is expected as the highest turbulence occurs near the canal bed in both configurations. Considering that the RS-90 fishway model overestimates flow velocities near the left sidewall (measuring points 6-8, see Figure 2 and Figure 9), it can reasonably be stated that fish could expend even less energy than presented in this paper for such configuration. For the RS-45 configuration, the lowest amount of energy the fish expends in its movement through the surface layer, while swimming in the mid-layer, results in the highest energy consumption.

However, it is important to note that the presented ABM simulation results should not be perceived as absolutely correct, but rather useful for comparing different fishway configurations.

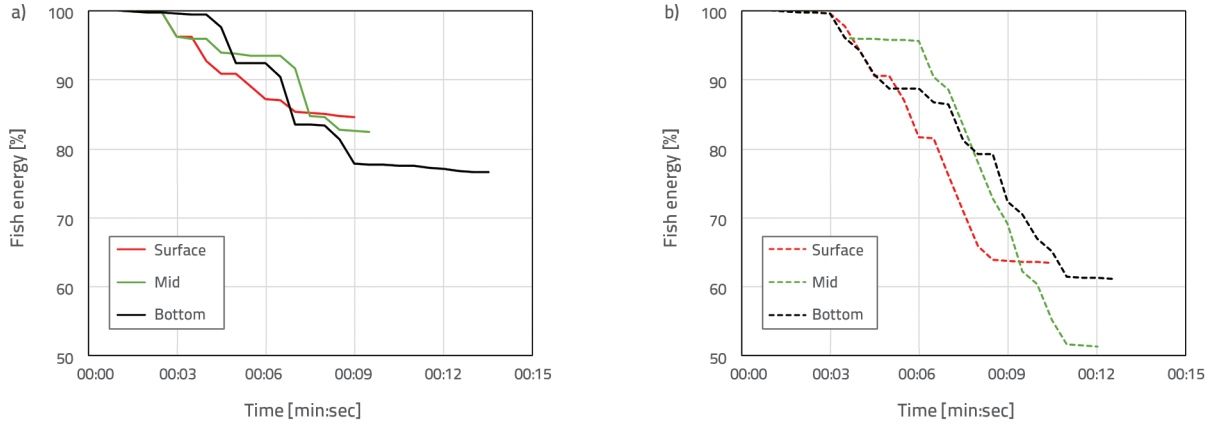

Figure 14. Fish energy loss rate during upstream movement through fishway (left – RS-90, right – RS-45) on the background of TKE field and flow velocity vectors for each σ-layer

4. Conclusion

Physical and 3D hydrodynamic numerical models were developed for two vertical slot fishway configurations while the numerical component was upgraded with the original ABM of the fish swimming upstream. The calibration and verification of the numerical model were conducted based on the measurements conducted on the physical model (9 measuring points in three layers). The results of past studies that examined fish behaviour in similarly configured fishways were used in the case of verification of the original ABM. The developed ABM considers the fish sensing ability as well as their cognitive aspect of reacting to the changes in their hydrodynamic ambient (flow direction and velocity, turbulence) in order to minimise the agent's energy consumption. Besides considering the abiotic factors, the basic motivation for the agent's movement is the assumed hormone field which is defined as a field monotonously increasing in the upstream direction. The results of six numerical simulations are presented in the paper, with one half relating to RS-90, and the other half to RS-45 configuration. The conducted simulations differ in the depth at which the agent is introduced into the model domain (surface layer, mid-layer, bottom layer).

The fish movement pattern is recognized based on the obtained agent's trajectories, from which it can be seen that the fish avoids the zones of high turbulence by adjusting swimming direction and speed depending on the changes in flow direction and velocity. Also, the agent's disorientation in the zones of rapid flow direction and velocity change is successfully modelled with the developed ABM. Such fish behaviour was recognized in previous studies performed on live individuals in altered flows. The results also show that the fishway with a greater distance between pool baffles exhibits more favourable flow conditions in terms of reducing the fish energy consumption. Although such conclusion is rather obvious and expected, the presented results quantitatively confirm this hypothesis. The advantage of longer pools in a fishway lies in the occurrence of recirculation zones in which a reversed flow is present (flow vector directed upstream). It can therefore be concluded that a fishway with a smaller number of longer pools provides a more favourable hydrodynamic environment for fish than the configuration with a greater number of shorter pools.

Past ABM studies were mainly related to the modelling of fish individuals as the agents with behavioural abilities who recognize the ambient abiotic factors, but the main objective was to find the fishway entrance. The results presented in this paper are rather useful in terms of improving the previous models and studies by applying the ABM principle in the analysis of fish swimming through differently configured fishways. Therefore, this paper gives an insight into another type of successful application of the ABM for solving real-life problems environmental engineering is concerned with.

It is important to note that mutual interaction between fish and flow is not considered within the developed ABM, which is mainly related to neglecting the changes in flow pattern due to the presence of a fish body. This mechanism could be significant in the regions of contracted flow in fishways, such as at baffle openings. In these regions, the flow area is significantly smaller than the cross-section of the recirculation zones. During the fish movement through the openings, the active cross-section is reduced, which results in the change of ambient velocity field and hydrodynamic drag. Therefore, further research should be focused on the improvement of the current ABM with the above-described component.

This paper presents a contemporary methodology for modelling typical physical processes on the example of a pilot model. It is certainly advisable to apply such an approach in fishway design procedures as an alternative to the formerly used conventional empirical templates.

Acknowledgements:

This research has been supported by the Croatian Science Foundation (DOK-2020-01) and ProtectAS project (KK 05.1.1.02.0013).

REFERENCES

[1] Jovanović, M.: Riblje staze u sklopu 'naturalnog' uređenja malih vodotoka, Vodoprivreda, 43 (2011) 4-6, pp. 217-226.

[2] PIANC: Fish passage, report n° 127, Bruxelles, Belgija, 2013.

[3] Ocvirk, E., Gilja, G., Jelić, D., Bujak, D., Cikojević, A., Đerek, I., Marić, M., Martinović, D.: Planiranje i projektiranje ribljih staza, Konačna studija, Sveučilište u Zagrebu, Građevinski fakultet, Zagreb, Republika Hrvatska, 2018.

[4] Web, P.W.: Hydrodynamics and energetics of fish propulsion, Bulletin of the Fisheries Research Bord of Canada, Information Canada, Ottawa, 1975.

[5] Beamish, F.W.H.: Swimming capacity (Chapter), Fish physiology, (eds. Hoar, W.S., Randall, D.J.), Randall, Academic Press, New York, pp. 101-187, 1978.

[6] Katopodis, C.: Developing a toolkit for fish passage, ecological flow management and fish habitat works, Journal of Hydraulic Research, 43 (2005) 5, pp. 451-467,

[7] Liao, J.C.: The role of the lateral line and vision on body kinematics and hydrodynamic preference of rainbow trout in turbulent flow, The Journal of Experimental Biology, 209 (2006), pp. 4077-4090, 10.1242/jeb.02487

[8] Liao, J.C.: The review of fish swimming mechanics and behaviour in altered flows, Philosophical Transactions of The Royal Society B: Biological Sciences 362 (2007) 1487, pp. 1973-1993, http://www.ncbi.nlm.nih.gov/pmc/articles/PMC2442850/ (10.02.2015.)

[9] Silva, A.T., Santos, J.M., Ferreira, M.T., Pinheiro, A.N., Katopodic, C.: Effects of water velocity and turbulence on the behaviour of iberian barbel (Luciobarbus Bocagei, Steindachner 1864) in an experimental pool-type fishway, River Research Application, 27 (2011), pp. 360.373, 10.1002/rra.1363

[10] Sokoray-Varga, B., Weichert, R., Lehmann, B., Nestmann, F.: Time-Resolved PIV Measurements to Investigate the Characteristics of the Turbulent Structures in a Vertical-Slot Fish Pass, The 9th International Symposium on Ecohydraulics, Beč, 2012.

[11] Calluaud, D., Pineau, G., Texier, A., David, L.: Modification of vertical slot fishway flow with a supplementary cylinder, Journal of Hydraulic Research, 52 (2014) 5, pp. 614-629.

[12] Calluaud, D., Cornu, V., Bourtal, B., Dupuis, L., Refin, C., Courret, D., David, L.: Scale Effects of Turbulence Flows in Vertical Slot fishways: Field and Laboratory Measurement Investigation, The 9th International Symposium on Ecohydraulics, Beč, 2012.

[13] Hockley, F.A., Wilson, C.A.M.E., Brew, A., Cable, J.: Fish responses to flow velocity and turbulence in relation to size, sex and parasite load, Journal of the Royal Society Interface, 11 (2014) 91, https://doi.org/ 10.1098/rsif.2013.0814

[14] Cai, L., Chen, J., Johnson, D., Zhiying, T., Huang, Y.: Effect of body length on swimming capability and vertical slot fishway design, Global Ecology and Conservation, 22 (2020), https://doi.org/ 10.1016/j.gecco.2020.e00990

[15] Fish, F.E.: Swimming Strategies for Energy Economy (Chapter), Fish Locomotion: An Eco-ethological Perspective, 2010., pp. 90-122, https://doi.org/ 10.1201/b10190-5.

[16] McKenzie, D.J.: Swimming and other activities - Energetics of Fish Swimming, Encyclopedia of Fish Physiology, 2011., pp. 1636-1644.

[17] Tarrade, L., Texier, A., David, L., Larinier, M.: Topologies and measurements of turbulent flow in vertical slot fishways, Hydrobiologia, 609 (2008), pp. 177-188.

[18] Bermudez, M., Rodriguez, A., Cea, L.: Implications of fish behavior for vertical slot fishways design, 9th International Symposium on Ecohydraulics ISE 2012, Beč, 2012.

[19] Li, Y., Wang, X., Xuan, G., Liang, D.: Effect of parameters of pool geometry on flow characteristics in low slope vertical slot fishways, Journal of Hydraulic Research, 58 (2020) 3, pp. 395-407, https://doi.org/ 10.1080/00221686.2019.1581666

[20] DeAngelis, D.L., Mooij, W.M.: Individual-based modeling of ecological and evolutionary processes, Annu. Rev. Ecol. Evol. Syst, 36 (2005), pp. 147-168.

[21] Grimm, V., Railsback, S.F.: Individual-Based Modeling and Ecology, Princeton University Press, Princeton, NJ., 2005.

[22] Macal, C.M., North, M.J.: Tutorial on agent-based modelling and simulation, Journal of Simulation, 4 (2010) 3, pp. 151-162

[23] Epstein, J.M.: Generative Social Science: Studies in Agent-Based Computational Modeling. Princeton University Press, Princeton, NJ., 2007.

[24] Goodwin, R.A., Anderson, J.J., Nestler, J.M.: Decoding 3-D movement patterns of fish in response to hydrodynamics and water quality for forecast simulation, 6th International Conference on Hydroinformatics, 2004., https://doi.org/ 10.1142/9789812702838_0031

[25] Goodwin, R.A., Nestler, J.M., Anderson, J.J., Weber, L.J., Loucks, D.P.: Forecasting 3-D fish movement behavior using a Eulerian-Lagrangian-agent method (ELAM), Ecological Modelling, 192 (2006), pp. 197-223, https://doi.org/ 10.1016/j.ecolmodel.2005.08.004

[26] FITHydro project - Agent based model, https://www.fithydro.wiki/index.php/Agent_based_model, 01.01.2021.)

[27] De Bie, J., Benson, T., Gaskell, J., Kemp, P.S.: Development and application of an agent based model for glass eel selective tidal stream transport, International Conference on Engineering and Ecohydrology for Fish Passage, cohydrology for Fish Passage. 12. https://scholarworks.umass.edu/fishpassage_conference/2018/December13/12

[28] Heinänen, S., Chudzinska, M.E., Mortensen, J.B., En Teo, T.Z., Utne, K.J., Sivle, L.D., Thomsen, F.: Integrated modelling of Atlantic mackerel distribution patterns and movements: A template for dynamic impact assessments, Ecological Modelling, 387 (2018), pp. 118-133, https://doi.org/ 10.1016/j.ecolmodel.2018.08.010

[29] Rodi, W.: Examples of calculation methods for flow and mixing in stratified fluids, Journal of Geophysical Research, 92 (1987) C5, pp. 5305-5328.

[30] Smagorinsky, J.: Some historical remarks on the use of nonlinear viscosities, Large eddy simulations of complex engineering and geophysical flows, (eds. Galperin, B., Orszag, S.), Cambridge University Press, pp. 1-34, 1993.

[31] Loubens, G.: Introduced species - Salmo gairdneri (Rainbow trout) (Chapter), Lake Titicaca - A Synthesis of Limnological Knowledge, (eds. Dejoux, C., Iltis, A.), Kluwer Academic Publishers, Dordrecht, pp. 420-426, 1992.

[32] DHI: MIKE ECO Lab - Numerical Lab for Ecological and Agent Based Modelling, User Guide, pp. 133, 2017.

[33] Wilkis, D.S.: Statistical methods in the atmospheric sciences, Second edition, Department of Earth and Atmospheric Sciences, Cornell University, 2006.

[34] Bermudez, M., Puertas, J., Cea, L., Pena, L., Balairon, L.: Balairon: Influence of pool geometry on the biological efficiency of vertical slot fishways, Ecological Engineering, 36 (2010), pp. 1355-1364, https://doi.org/10.1016/j.ecoleng.2010.06.013

[35] Marriner, B.A., Baki, A.B.M., Zgu, D.Z., Cooke, S.J., Katopodis, C.: The hydraulics of a vertical slot fishway: A case study on the multi-species Vianney-Legendre fishway in Quebec, Canada, Ecological Engineering, 90 (2016), pp. 190-202, https://doi.org/10.1016/j.ecoleng.2016.01.032